

See discussions, stats, and author profiles for this publication at: <https://www.researchgate.net/publication/332784647>

Biodegradability Study by FTIR and DSC of Polymers Films Based on Polypropylene and Cassava Starch

Article in *Orbital - The Electronic Journal of Chemistry* · April 2019

DOI: 10.17807/orbital.v1i12.1360

CITATIONS

0

READS

460

4 authors:



Arturo Bismarck Linares Veliz

Universidade Federal do Rio Grande do Sul

3 PUBLICATIONS 0 CITATIONS

SEE PROFILE



Juan Carlos Jiménez García

National University of Cordoba, Argentina

5 PUBLICATIONS 0 CITATIONS

SEE PROFILE



Pedro Lopez

Universidad de Oriente, Nucleo Nueva Esparta

7 PUBLICATIONS 6 CITATIONS

SEE PROFILE



Blanca Rojas de Gáscue

Universidad de Oriente (Venezuela)

105 PUBLICATIONS 263 CITATIONS

SEE PROFILE

Some of the authors of this publication are also working on these related projects:



Driving the Next Product Innovation via Hydrogels [View project](#)



Proporcionar apoyo al Servicio de Traumatología del Hospital Universitario Antonio Patricio Alcalá (HUAPA) de Cumaná para evaluar la calidad de los Biomateriales que emplean y proponer nuevos desarrollos [View project](#)

Biodegradability Study by FTIR and DSC of Polymers Films Based on Polypropylene and Cassava Starch

Arturo Bismarck Linares^{*a}, Juan Carlos Jiménez^a, Pedro López^b, and Blanca Rojas de Gásque^a

^aLaboratorio de Polímeros. Instituto de Investigaciones en Biomedicina y Ciencias Aplicadas "Dra. Susan Tai". Universidad de Oriente. Avenida Universidad, Cerro del Medio. Cumaná 6101 Estado Sucre, Venezuela.

^bCentro Regional de Investigaciones Ambientales. Universidad de Oriente. Avenida 31 de julio Guatamare 6301, Estado Nueva Esparta, Venezuela

Article history: Received: 31 October 2018; revised: 18 March 2019; accepted: 20 March 2019. Available online: 07 April 2019. DOI: <http://dx.doi.org/10.17807/orbital.v11i2.1360>

Abstract:

The polypropylene resistance to biological attacks is related to the lack of functional groups recognizable by microbial enzymatic systems. The incorporation of compatibilizing agents in polypropylene (PP)/starch (S) blends favors the interactions of their components and can potentially induce the material degradation. In order to study the degradation of PP/S blends, films were prepared with a compatibilizing agent (AC), constituted by polypropylene grafted with acrylamide (PP-g-AAm). The films were placed in an Erlenmeyer flask containing 100 mL of a basal mineral medium with microorganisms inoculated in a cellulose filter, taken from an effluent. The FTIR analyzes of the films with the AC agent showed significant differences in the absorption bands, with respect to the control film. The asymmetric stretch signal of the grafted acrylamide that appeared at 3292 cm^{-1} increased in intensity only in the inoculated blends. In addition, hydrolysis was evidenced by the stretching signal of the OH bond. Abrupt changes were observed in the carbonyl region ($1700\text{-}1600\text{ cm}^{-1}$) with the appearance of new bands, which shows the rupture of polymer chains. In the blends DSC analysis, a slight nucleation effect is observed in addition to a considerable increase in the degree of crystallinity, so it is suggested that the degradation could be occurring in the amorphous regions.

Keywords: biodegradation; blends; polypropylene starch

1. Introduction

In recent years, the growing environmental conscience has encouraged the development of biodegradable materials from renewable resources to replace conventional non-biodegradable materials in many applications [1]. This material must consider two requirements: maintaining physical and mechanical properties required by a plastic product and exhibit biodegradability characteristics [2]. Among them, polysaccharides such as starches offer several advantages for the replacement of synthetic polymers in plastics industries due to their low cost, non-toxicity, biodegradability and availability, which can be a way to solve the

problem of pollution [3]. Starch is a renewable, biodegradable hydrophilic polymer that has been employed as filler in blends with different synthetic materials up to a certain amount [4].

It is a semi-crystalline polymer composed of linear polysaccharide molecules (amylose) and branched molecules (amylopectin). It is a natural polymer stored in the form of granules in several plants which is an inexpensive, versatile and available material [5]. Disrupting starch granules in presence with glycerol by conventional processing equipment can lead to thermoplastic starch (TPS) [6]. Starch can be blended with various synthetic and natural polymers. But, in the case of polyolefins like polypropylene, the high interfacial tension when it is blending with starch

*Corresponding author. E-mail: bismarck1989@gmail.com

must be reduced in order to ensure homogeneity at microscopic level, due to blends can deteriorate [7]. In order to overcome these drawbacks, two steps can be followed: modify the starch before blending it, or add a compatibilizing agent that improves the polyolefin/starch blends [8]

A process of stabilization in polymer blends can be carried out through chemical processes that generate a compatibilization between the components of the blend with the inclusion of small quantities of compatibilizers. With the introduction of reactive functional groups in the apolar polymer chain, coupling of organic molecules can be generated by specific interactions, such as hydrogen bonds or covalent bonds [9]. In order to achieve this, the use of a modified polypropylene as a component of the blend offers an approach to meet the performance requirements. Rivero et al., 2008, has reported studies on blends prepared with Lineal Low Density Polyethylene (LLDPE) and octenyl succinate modified starch. These modified starches could find application as compatibilizers in LLDPE/S blends [10]. Modification of starch with alkenyl succinic anhydrides has been of interest because this modification disrupts hydrogen bonding between starch molecules and reduces its retrogradation, while imparting an amphiphilic character [11].

Some studies have shown the partial degradation of polymers such as polyethylene (PE) with UV irradiation, thermal treatment or oxidation with nitric acid, as well as the use of surfactants, which facilitate the formation of a biofilm on the surface of the PE, increasing thus its affinity with water [12]. The degradative process can be summarized in two stages: an abiotic degradation and a biotic attack. Pro-oxidant additives, also called pro-degradants, are used to generate an accelerated fragmentation of the plastic material with the aim of decreasing its molecular mass, the size of the polymer chains, its hydrophobic character and for the formation of lighter compounds and labile to the metabolisms of microbial organisms, such as bacteria, fungi and algae, all with the aim of facilitating their bioassimilation after the abiotic degradation process [13-15].

Recent research shows the influence of different thermoplastic starch (TPS) contents on LLDPE matrices and the morphology, mechanical

and thermal properties of blend changes with the increasing quantity of TPS. The biodegradation test shows that about 9% (w/w) of film is degraded in compost soil for 150 days [16]. The effect of blending corn starch and cassava starch with polypropylene has also been studied. This blend of starches has significant effects on the mechanical properties of PP when subjected to the action of microorganisms, the PP experienced a considerable decrease in its molar mass showing poor mechanical properties [17]. On the other hand, it has been reported that the properties of PP are influenced by the crystallization kinetics during cooling [18]. In this work were prepared blends of polypropylene and cassava starch, adding PP-g-AAm as compatibilizing and the most important of this study is to promote the degradation of polypropylene by adding cassava starch. The PP after of its interaction with microorganisms is characterized by FTIR and DSC study.

2. Results and Discussion

2.1 Characterization by Fourier-transform infrared spectroscopy (FTIR) of modified polypropylene

Polypropylene was characterized by FTIR to verify that new characteristic bands of the grafted monomers were generated. Figure 1 shows the FTIR spectrum of the polypropylene before and after being grafted with the polar acrylamide monomer (AAm), using 25% by mass of AAm with respect to the PP. The functionalization of PP with acrylamide monomer (PP-g-AAm) is appreciated with the appearance of new absorption bands that are not observed in pure PP and that are characteristic of acrylamide. The absorption band to 635 cm^{-1} is assigned to bending out of the plane of the N-H bond. While the absorption band a 1661 cm^{-1} has been assigned to the elongations of the carbonyl group C=O while at 3355 and 3170 cm^{-1} , the bands are assigned to the asymmetric and symmetric elongation vibrations of the N-H group characteristic of the primary amide.

Due to the importance of the band corresponding to the carbonyl group to the possible interaction with the hydroxyl groups of anhydroglucose units of the starch, the deconvolution technique was used to clarify the overlapping effect of the bands, where the

contribution of each one of them can be separated. In Figure 2, a signal at 1661 cm^{-1} can be seen which is mainly associated with the vibration of the amide carbonyl group, while the band at 1617 cm^{-1} can be related to the flexion vibration of the bond N-H and with the vibration of

the C-N bond. However, the band at 1617 cm^{-1} can also be assigned to stretches bonds -CH=CH₂, which would be evidence that, in addition to functionalization, collateral reactions of disproportion that are generating unsaturation in the PP chain.

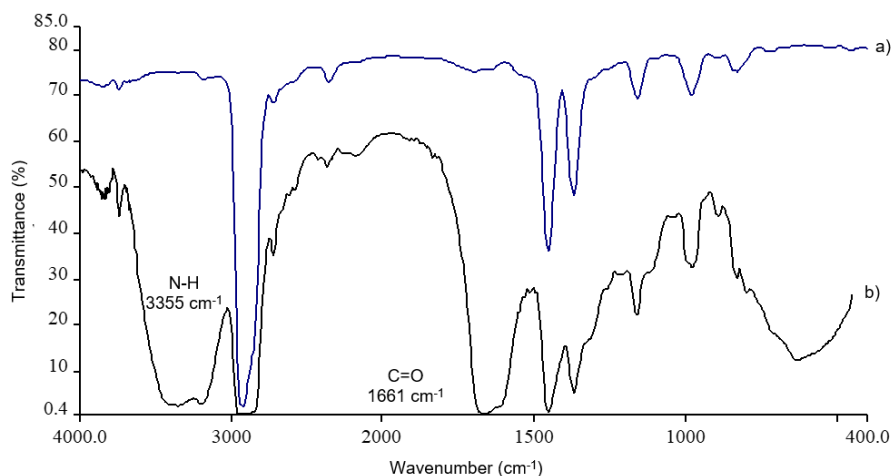


Figure 1. FTIR spectra of: (a) PP (b) PP-g-AAm.

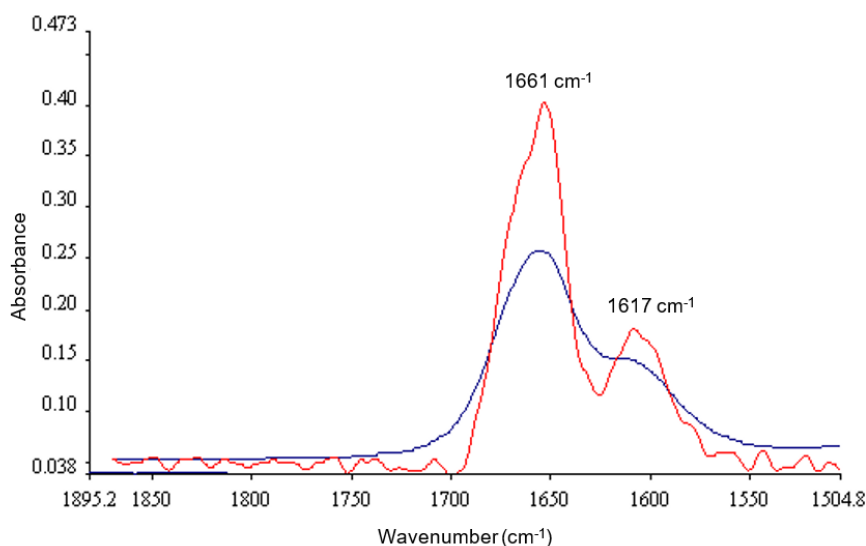


Figure 2. FTIR spectrum in absorbance mode with deconvolution of PP-g-AAm between 1890-1500 cm^{-1} . (Red: deconvoluted spectrum, Blue: absorbance spectrum).

By increasing the AAm content, the grafting of the monomer to the tertiary carbon is favored before the β break occurs. The signals of the AAm grafted at the ends of the chain with a double bond, increased markedly with the increase in AAm content, which indicated that the β break occurs after the AAm graft at the tertiary carbon. Figure 3 shows the reaction mechanism proposed in this research.

Once the presence of the functional groups was corroborated, was determined the degree of substitution (DS). DS indicates the number of functional groups grafted in the polypropylene chain in %mol. For the determination of the DS, a calibration curve was used reported by Nachtigall *et al.*, (Figure 2) for polypropylene functionalized with maleic anhydride [19]. A table 1 shows the degree of substitution using AAm monomer.

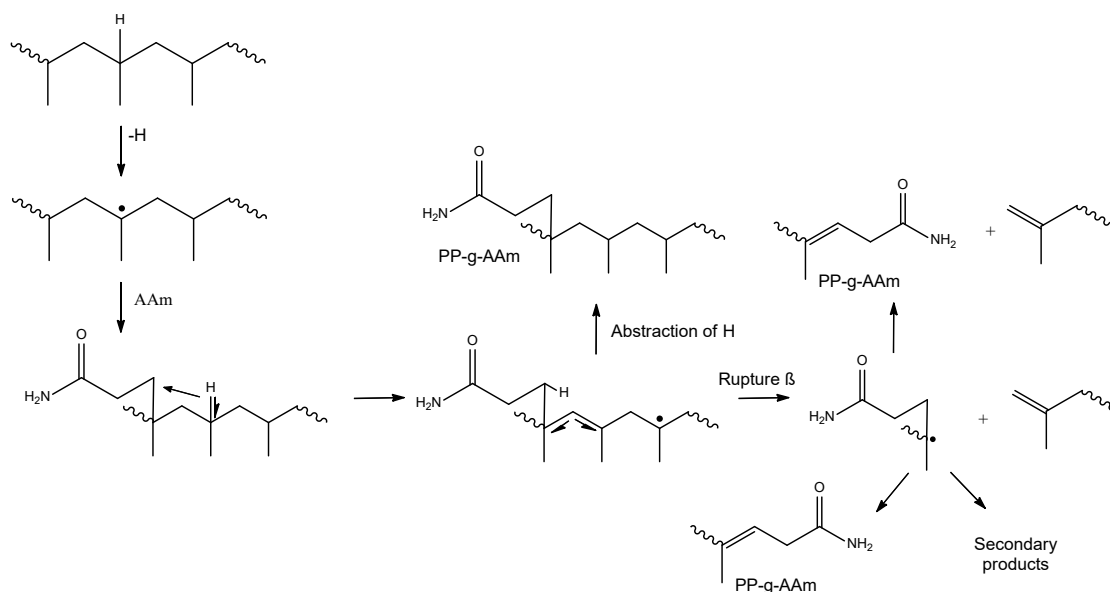


Figure 3. Schematic representation of the reaction that takes place between polypropylene and acrylamide.

Table 1. Degree of substitution (DS) obtained for the polypropylene.

Sample	$A_{c=O}/A_{1156cm^{-1}}$	Average DS (%mol)
PP-g-AAm	4.2518	7.1778±0.001

These results show a low degree of substitution obtained for the PP with respect to the amount of monomer grafted in the reaction and research reported previously in the modification of polyolefins such as polyethylene (PE) [9]. This can be attributed to the fact that the isotactic sequences of the PP, due to the effect of electronic repulsion, are hindering the insertion of the AAm into the polymer chain or possibly forming collateral reactions, such as acrylamide oligomers. However, the chemical modification of the PP was effective as corroborated in the FTIR spectra.

2.2 Thermal analysis of materials by Differential Scanning Calorimetry (DSC)

The calorimetric study allowed determining the crystallization exotherms and the fusion endotherms where the ordered or crystalline zones decrease. Table 2, Figures 4 show the thermal analysis of polypropylene functionalized with acrylamide (PP-g-AAm), where during the crystallization a decrease in the peak crystallization temperature (T_c) was observed at 2 °C and a decrease at 3 °C in the peak melting temperature with respect to polypropylene, which indicates that the polar groups of acrylamide grafted in the PP, are hindering its dynamic crystallization from the melt, also affecting the melting temperature, confirming the results obtained by FTIR.

Table 2. Thermal Properties of PP and PP-g-AAm.

Sample	T_c onset (°C)	T_c (°C)	ΔH_c (J/g)	T_m onset (°C)	T_m (°C)	ΔH_m (J/g)	(1- λ)
PP	125.1	120.9	-83	150.5	163.1	83	40
PP-g-AAm	114.3	118.5	-64	150.6	160.7	67	33

T_{co} : onset temperature, T_c : crystallization temperature, ΔH_c : enthalpy of crystallization, T_{mo} : onset melting temperature, ΔH_m : enthalpy of melting and (1- λ): degree of crystallinity.

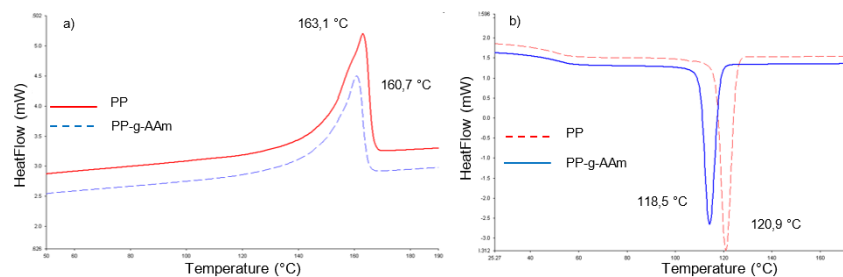


Figure 4. DSC curves of polypropylene grafted with acrylamide: a) melt temperature (T_m) b) crystallization temperatures (T_c).

2.3 PP/Starch blends

2.3.1 Characterization by FTIR and Thermal Properties

Figure 5 shows characteristic bands of polypropylene, mainly the bands assigned to the asymmetric elongation of the CH bonds (ν_{as}) to 2923 cm^{-1} , to 1455 cm^{-1} bending vibrations attributed to the asymmetric deformations (δ_{as}) of the CH bond of the group CH_2/CH_3 and symmetric bending vibrations (δ_s) assigned to the C-H vibrations of the CH_3 group to 1370 cm^{-1} . In addition, characteristic bands of the OH group to 3421 cm^{-1} as well as bands corresponding to the C-C stretches ($575, 765, \text{ y } 862\text{ cm}^{-1}$) and to the C-H vibrations ($\nu_{\text{C-C}}$: $800\text{--}1200\text{ cm}^{-1}$, $\delta_{\text{C-H}}$: $1300\text{--}1450\text{ cm}^{-1}$, $\nu_{\text{C-H}}$: $2000\text{--}3400\text{ cm}^{-1}$) presents in the structure of the starch. The amylose molecules contain hydroxyl groups that can form hydrogen bonds and generate hydrated micelles. This characteristic is observed in the 1648 cm^{-1} band, which has been attributed to the water that is associated in the starch [10]. The absence of new bands or notable changes in the bands of the components confirms the non-compatibility of the blend.

The relevant transition temperatures and enthalpies extracted from the cooling runs performed in the DSC after erasing thermal history and the subsequent heating runs for PP/S and PP/S/PP-g-AAm blends ($DS=7,2$), shows table 3 and the DSC thermograms of samples, refer to the second heating. An unfavorable interaction between the molecular segments of the components results in a high interfacial tension in the molten state, which hinders the formation of a finely dispersed phase.

Figure 6 show the PP/S blend (60/40) experienced an increase of $2\text{ }^\circ\text{C}$ in the crystallization temperature with respect to the PP. The thermal properties of PP are influenced by the kinetics of crystallization during cooling and the increase [20] in T_{∞} and T_c indicates that the starch is acting as a heterogeneous nucleating agent. Figure 7 show the variations in the crystallization temperature (T_{∞} , T_c), in the T_m and a decrease in the degree of crystallinity of PP/S/PP-g-AAm blend (90/10/1). These results indicate that the compatibilizing agent could be exerting a more effective nucleation action in the blends with a lower proportion of starch compared to the non-compatibilized blends. Figure 8 shows the FTIR spectra of PP/S blends with PP-g-AAm.

Table 3. Thermal Properties of blends.

Sample	T_{∞} ($^\circ\text{C}$)	T_c ($^\circ\text{C}$)	ΔH_c (J/g)	T_{mo} ($^\circ\text{C}$)	T_m ($^\circ\text{C}$)	ΔH_m (J/g)	(1- λ)
PP/S							
100/0	125.1	120.9	-83	150.5	163.1	83	40
90/10	125.1	120.9	-81	153.9	164.7	70	38
80/20	123.3	119.6	-59	155.9	163.4	58	35
70/30	123.3	119.6	-60	154.2	164.4	60	41
60/40	126.4	122.3	-46	154.7	165.4	48	38
PP/S/PP-g-AAm							
90/10/1	125.9	122.3	-76	155.3	164.5	77	41
80/20/2	125.1	121.3	-49	155.8	164.7	57	34
70/30/3	122.2	118.3	-57	152.6	162.1	58	40
60/40/4	123.4	119.6	-49	152.9	163.1	53	43

T_{∞} : onset temperature, T_c : crystallization temperature, ΔH_c : enthalpy of crystallization, T_{mo} : onset melting temperature, ΔH_m : enthalpy of melting and (1- λ): degree of crystallinity.

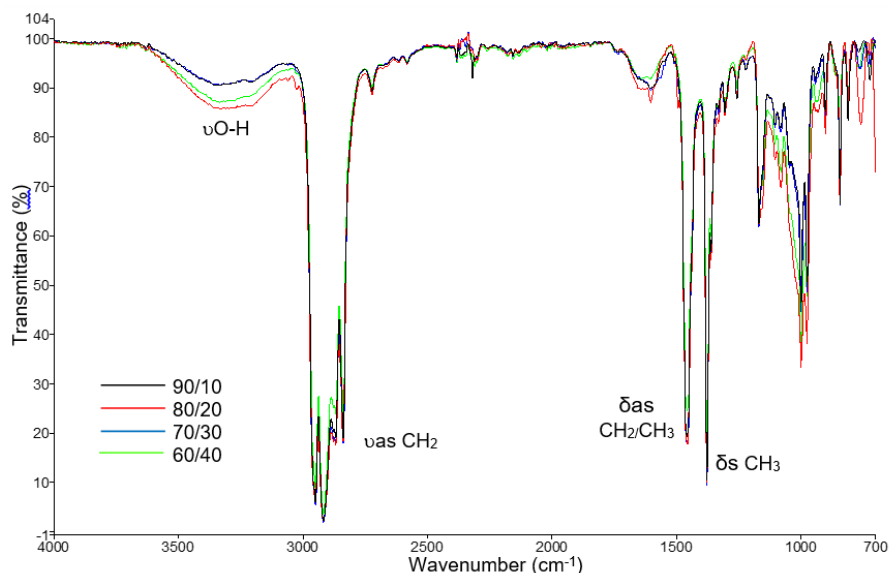


Figure 5. FTIR spectra of PP/S blends.

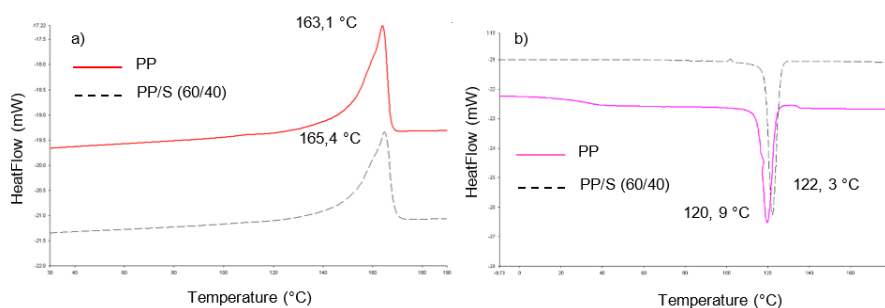


Figure 6. DSC curves of polypropylene/starch blends PP/S (60/40): a) melt temperature (T_m) b) crystallization temperatures (T_c).

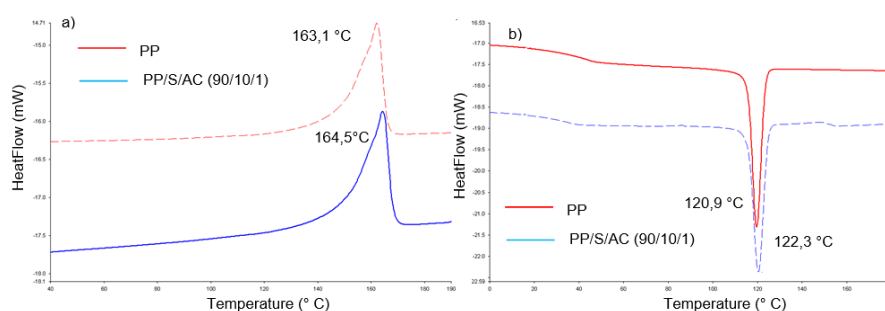


Figure 7. DSC curves of polypropylene/starch blends with compatibilizing agent PP/S (90/10/1): a) melt temperature (T_m) b) crystallization temperatures (T_c).

These results point to postulate there are interactions between the amino group of acrylamide and the OH present in the anhydroglucose units of starch. The OH band characteristic of the polysaccharide at 3300 cm^{-1} disappeared and the band of the carbonyl group of the grafted amide is displaced at lower

frequencies in the infrared spectrum in the blends 90/10/1 and 80/20/2 (figure 9), which evidences the presence of new interactions that affects the vibration of these bonds.

Therefore, the results allow to infer that the PP-g-AAm is acting as a bridge between the phases of the starch and of the polypropylene in particular

in the blends 90/10/1 and 80/20/2, generating hydrogen bonds between the starch and the acrylamide how is showed in a figure 10.

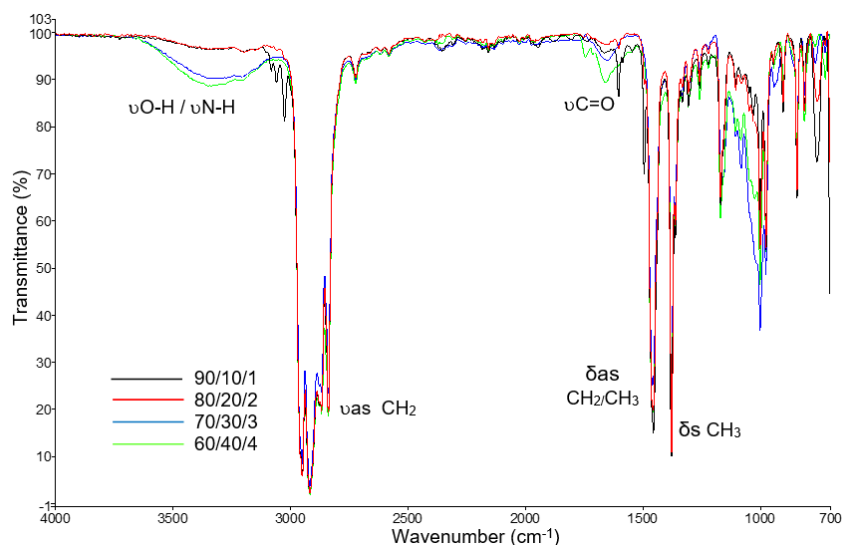


Figure 8. FTIR spectra of PP/S/PP-g-AAm blends.

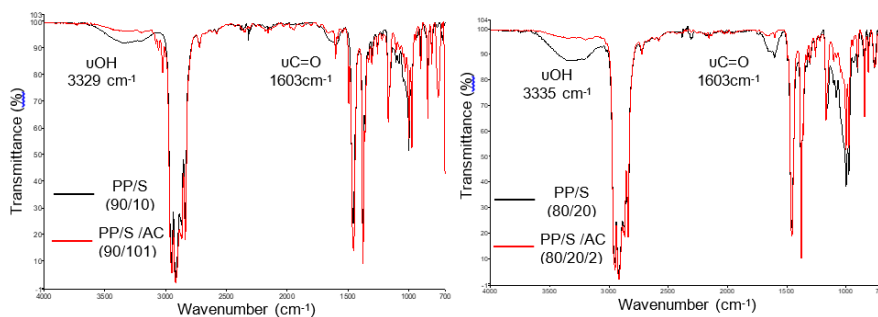


Figure 9. FTIR comparative spectra of PP/S and PP/S/PP-g-AAm blends.

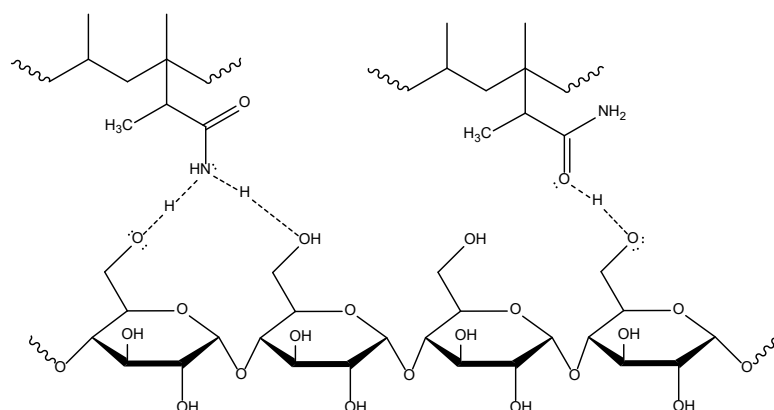


Figure 10. Hydrogen bond interaction between the OH of the anhydroglucose units and the C=O and NH₂ groups in the acrylamide grafted in the PP.

2.4 Biodegradability Test

2.4.1 Characterization by FTIR

PP/S, PP/S/PP-g-AAm blends with higher

amount of starch (60/40, 60/40/4) were evaluated in a basal mineral medium inoculated with microorganisms respect to those in control (medium without microorganisms). The spectra of

the blends 60/40 (figure 11) show an increase in the intensity of the absorption bands of the samples. From these results it can be inferred

that the interaction between the medium and the hydrophilic blends components has been favored with the hydrolysis and degradation of starch.

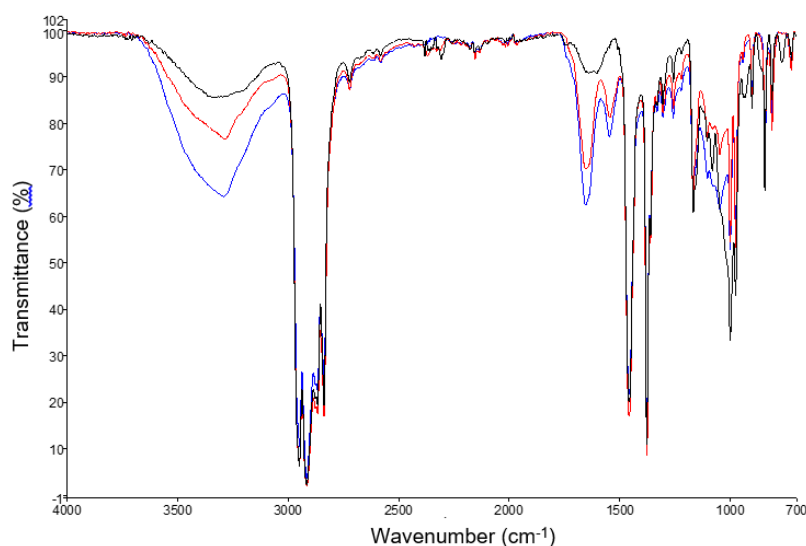


Figure 11. Comparative spectra of biodegradability test of PP/S (60/40) blend: Initial blend (black), in a basal mineral medium (red) and a basal mineral medium inoculated with microorganisms (blue).

The spectra of the blends 60/40/4 (figure 12) with the amide grafted in the PP show the stretching signal of the amide present in the blend with compatibilizing agent increased its intensity becoming a sharper band, where the overlap with the vibration of the ν OH was lower and only in the inoculated blends, evidencing the hydrolysis by the stretching signal of the O-H bond. This was corroborated by a peak that appeared at

approximately 1050 cm^{-1} , a signal that did not appear in the control blend. A signal was also detected at 998 cm^{-1} assigned to the vibrations of the chain. The chemical structure of cassava starch and the compatibilizing agents containing functional groups along the chain make the blend more susceptible to attack by the basal medium and microorganisms, since these bonds are susceptible to hydrolytic degradation, as has been reported by other authors [21].

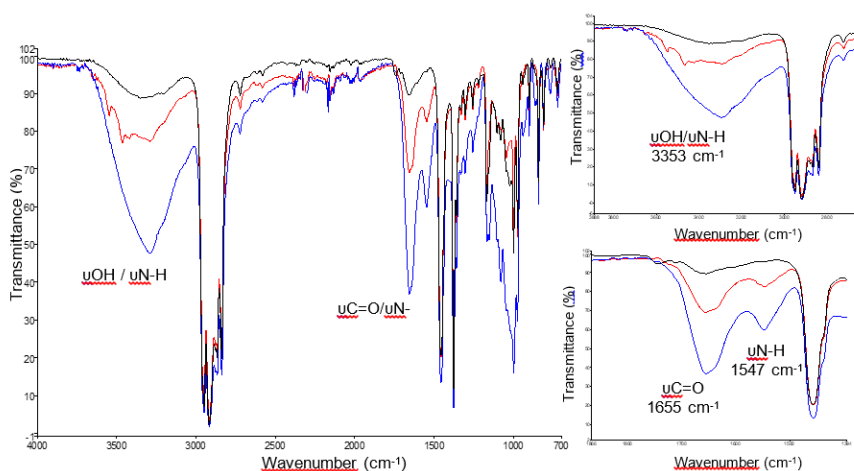


Figure 12. Comparative spectra of biodegradability test of PP/S/PP-g-AAm (60/40/4) blend: Initial blend (black), in a basal mineral medium (red) and a basal mineral medium inoculated with microorganisms (blue).

The spectra showed that Blends are being hydrolyzed, in this sense changes were observed

in the carbonyl group region ($\text{C}=\text{O}$) between $1750\text{--}1650\text{ cm}^{-1}$. From the results obtained in the

blends characterization in FTIR, it can be inferred that the medium favors hydrolysis in the blends and that the inoculated microorganisms act as catalysts of the degradative process, due to the increase in the OH bond signal to 3353 cm^{-1} . Furthermore, it is proposed that the amides of the compatibilizing agent and the starch may be being hydrolyzed by the increase in the intensity of the N-H bands to 1547 cm^{-1} and the C=O area to 1655 cm^{-1} corresponding to the products derived from the hydrolysis. This phenomenon was due to an increase in the concentration of extracellular enzymes that are produced during the growth of bacterial consortium and that ultimately facilitate the degradation and its hydrolysis [22]. Previously, it was reported that *Bacillus spp.*, being producers of oxido reductases (extracellular enzymes), are capable of acclimatizing in

nutrient starving conditions during the degradation process [21]. This indicated the increase in concentrations of carbonyl and hydroxyl groups.

2.4.2 Thermal Properties

The biodegradation of polymers by microorganisms can be catalyzed by extracellular and degradative enzymes, which attack the macromolecular substrate giving rise to products of low molecular mass soluble in water [23, 24]. The attack consists of an enzymatically catalyzed hydrolytic process where the enzymes attack groups susceptible to hydrolysis [25]. Table 4 shows the relevant transition temperatures and enthalpies from blends after biodegradability test.

Table 4. Thermal Properties of blends before and after the biodegradability test in a basal mineral medium inoculated with microorganisms (mic) and without microorganisms (ctrl).

Sample	T_{co} (°C)	T_c (°C)	ΔH_c (J/g)	T_{mo} (°C)	T_m (°C)	ΔH_m (J/g)	(1- λ)
PP/S							
60/40	126.4	122.3	-46	154.7	165.4	48	38
60/40ctrl	128.4	125.3	-57	153.8	165.1	53	43
60/40mic.	128.5	125.5	-66	153	164.8	54	43
PP/S/PP-g-AAm							
60/40/4	123.4	119.6	-49	152.9	163.1	53	43
60/40/4ctrl	129.6	126.9	-83	152.8	164.5	83	67
60/40/4mic.	129.4	126.5	-93	151.1	164.3	95	76

T_{co} : onset temperature, T_c : crystallization temperature, ΔH_c : enthalpy of crystallization, T_{mo} : onset melting temperature, ΔH_m : enthalpy of melting and (1- λ): degree of crystallinity.

Figure 13-16 show comparative DSC curves of biodegradability test of blends. ΔH_m tends to increase in the blends, especially blends with compatibilizing agent. These changes in ΔH_m (and therefore in the degree of crystallinity), are mainly due to the cleavage of the bonds located in the amorphous region of the PP. Such chain scission results in a decrease in tangles in segments and allows an increase in crystallinity to occur in the remaining segments [23]. The amorphous and crystalline fraction of a polymer does not necessarily degrade at the same rate. At longer degradation times, greater degradative breakdown activity can then occur in the crystalline regions of the different systems indicated. The damage in the crystalline zones will affect initially those thinner crystals and this could gradually destroy this region until at very long degradation times the thickest crystals will be attacked. This increase in the degree of

crystallinity is due to the degradation in polymers occurring faster in the amorphous regions than in the crystalline regions, and when the amorphous regions have been removed, it is when the degradative stage begins that it will affect the crystalline zones [23, 25].

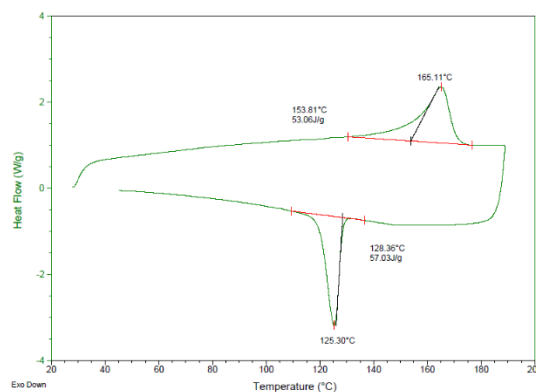


Figure 13. Comparative DSC curves of biodegradability test of PP/S (60/40) blend in a basal mineral medium.

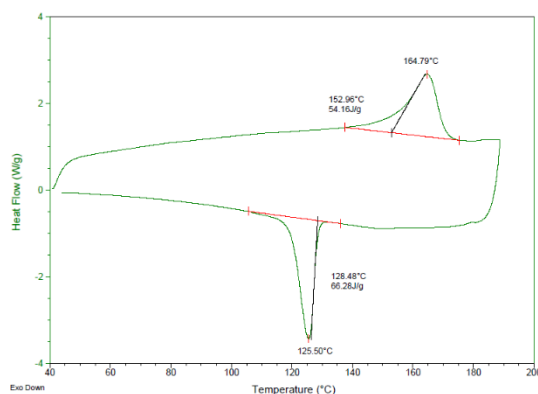


Figure 14. Comparative DSC curves of biodegradability test of PP/S (60/40) blend in a basal mineral medium inoculated with microorganism.

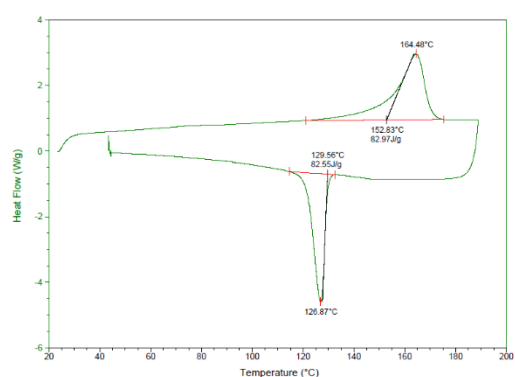


Figure 15. Comparative DSC curves of biodegradability test of PP/S/PP-g-AAm (60/40/4) blend in a basal mineral medium.

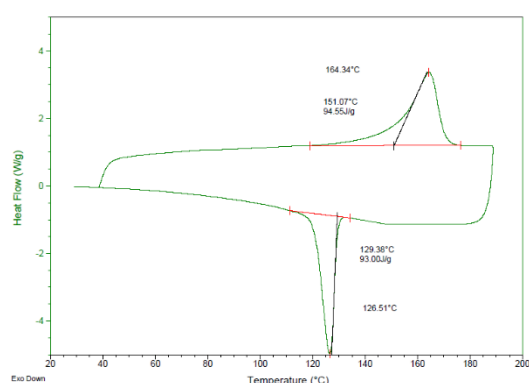


Figure 16. Comparative DSC curves of biodegradability test of PP/S/PP-g-AAm (60/40/4) blend in a basal mineral medium inoculated with microorganism.

3. Material and Methods

3.1 Materials

In this research was used a commercial polypropylene (PP) grade J-846, (13.9%

ethylene) produced by the company PROPILVEN (located in the petrochemical complex "Ana Maria Campos", Zulia State, Venezuela), which is employed in the injection of thin wall parts or with intricate design. The cassava starch was donated by the Polymer Group of the Universidad Simón Bolívar, its origin is from the subsidiary of PDVSA San Tomé INVEYUCA. For the PP functionalization was used a polar monomer acrylamide (AAm) and a free radical initiator, the benzoyl peroxide.

3.2 Preparation of compatibilized agent (PP-g-AAm)

This reaction was carried out following the procedure described by Rojas de Gáscue *et al.*, to obtain the functionalized polypropylene (PP), 25% of the acrylamide monomer (AAm) was used with respect to the PP. For this, in a three-necked flask under an inert nitrogen atmosphere, 3 g of PP were placed in 67 mL of o-dichlorobenzene with magnetic stirring at a temperature of 150 °C. After complete dissolution of the polymer, 0.75 g of AAm was added to obtain the PP-g-AAm and 0.07 g of the free radical initiator benzoyl peroxide (BP). After that moment, the reaction time was counted until completing 67 min [9]. The product was precipitated in 100 mL of acetone with magnetic stirring and subjected to an exhaustive Soxhlet extraction with acetone for 9 h. Finally, the product was dried in a vacuum oven at 60 °C for 12 h.

3.3 Blends preparation.

Polypropylene/native cassava starch blends (100/0, 90/10, 80/20, 70/30, and 60/40), PP/S blends, were prepared by melt-extrusion. Previously, the starch dried under vacuum at 40 °C for 48 h. The mixing was performed in an ATLAS laboratory scale screw extruder (ATLAS CS-194) between 160-190 °C and with a screw speed of 60 rpm. PP was processed once before preparing the blends and, then, each blend was extruded three times to improve homogeneity. Finally, the extruded filaments were cut into pellets. PP/S/PP-g-AAm blends with the following compositions were prepared: 90/10/1, 80/20/2, 70/30/3, 60/40/4, where the amount of PP-g-AAm was always 10 wt.% with respect to the disperse phase of native cassava starch. Before the

extrusion of the blends, PP-g-AAm and native starch were blended manually in a first step. Melt-extrusion of these blends was carried out under the conditions previously indicated for LLDPE/S blends [10].

3.4 Biodegradability test

In this study, the biodegradability of films is investigated with membrane filtration method. Films PP/S, PP/S/PP-g-AAm (60/40 and 60/40/4) respectively were selected, since they have the highest content of cassava starch. Pellets were taken from the blends and films were prepared in a Carver brand hydraulic press. The source of the microorganisms was an effluent originating in a hotel in Margarita Island, Venezuela. Analysis effluent indicated that it was rich in *Enterobacteriaceae* (*Escherichia coli*), *Pseudomonaceae* (*Pseudomonas aeruginosa*), *Vibrionaceae* (*Vibrio cholera*) and *Bacillaceae* (*Bacillus sp*). From this effluent 20 mL were used for each Erlenmeyer flask. The basal mineral medium was prepared by dissolving in one liter of distilled water the following mineral salts: NH_4Cl , $\text{MgSO}_4 \cdot 7\text{H}_2\text{O}$, NaCl , $\text{FeSO}_4 \cdot 7\text{H}_2\text{O}$ and K_2HPO_4 and the pH was adjusted to 7.2 ± 0.2 . Blends were placed in the form of sheets in Erlenmeyer flasks with 100 mL of the basal medium in the presence and absence of the microorganisms. A membrane filtration was performed to concentrate the microorganisms present in a cellulose filter with a mesh size of $0.45 \mu\text{m}$ and a diameter of 47 mm. Each filter was removed from the funnel to be placed in each Erlenmeyer flask. The samples were taken to an oven at 37°C for 75 days.

3.5 Fourier transforms infrared (FTIR) spectroscopy

Films from test biodegradability were directly analyzed by FTIR and Attenuated Total Reflection (ATR). The equipment was previously calibrated with polystyrene. FTIR spectra were recorder with a Perkin Elmer Spectrum model Frontier with a resolution of 2 cm^{-1} , 24 scans and wave number range between 400 and 4000 cm^{-1} . The data were analyzed by using the program Perkin Elmer Spectrum version 10.4.00. Discs were obtained by mixing dried starch with analytical grade KBr.

3.6 Determination of the degree of substitution (DS)

DS is the average of carbonyl groups substituted on polypropylene chain. The DS of AAam polypropylene (PP-g-AAm) was determined in an FTIR spectrophotometer and in the absorbance spectrum as a function of the wave number, the area under the curve comprised between 1700 and 1800 cm^{-1} corresponding to the vibration of the carbonyl group was integrated and also the existing one at 1156 cm^{-1} that belongs to the vibration of the methylene groups. The relationship between these areas is known as the carbonyl index (Ic) [19]. It was graphed according to the molar percentage (%mol) of AAam fed, constructing a calibration curve. Finally, the PP-g-AAm was treated under the same conditions of the standards to calculate the $A_{\text{C=O}}/A_{1156}$ ratio, and by extrapolation, the degree of functionalization of AAam in the polymeric chain of the PP is determined. DS was determined as follows.

$$\text{DS}(\% \text{mol}) = 1.6898 (A_{\text{C=O}}/A_{\text{CH}_3}) - 0.0069 \quad (1)$$

3.7 Differential Scanning Calorimetry (DSC)

Samples for differential scanning calorimetry (DSC) were punched from the compression-molded sheets. Small disc samples were cut ($5.0 \pm 0.2 \text{ mg}$) and encapsulated in aluminum pans. A Perkin- Elmer DSC-7 was used to study the thermal behavior of all compositions under ultra high purity nitrogen atmosphere. The instrument was calibrated with indium (T_m : 156.6°C ; ΔH : 28 J/g). "Standard" scans were performed by heating the samples since 25°C at 190°C for 3 min. Then they were cooled down to -10°C at $20^\circ\text{C}/\text{min}$ and finally they were heated from -10°C to 190°C at $20^\circ\text{C}/\text{min}$. The scans refer to the second heating. Melt temperature (T_m), enthalpy of fusion (ΔH_m) and crystallization temperature (T_c) were determined from DSC curves. The crystallinity degree ($1-\lambda$) of PP grafted with acrylamide is calculated using the following equation:

$$(1 - \lambda) = \frac{\Delta H_m}{\Delta H_m^\circ} \times 100 \quad (2)$$

where ΔH is the enthalpy of fusion, obtained from DSC curve, (ΔH_m is the enthalpy heat of 100% crystalline PP (207 J/g) [26]. In the case of determine the degree of crystallinity blends ($1-\lambda$)

the starch fraction present in the blend, is calculated using the following equation:

$$(1 - \lambda) = \frac{\Delta H_m}{\Delta H_m^\circ \times W_c} \times 100 \quad (3)$$

4. Conclusions

The chemical modification of polypropylene (PP) was achieved using acrylamide, where PP-g-AAm is acting as a bridge between the phases of the starch and the PP in the blends 90/10/1 and 80/20/2, generating interactions of hydrogen between starch and acrylamide. In the FTIR spectra increases in the area of the OH groups and the changes in the region of the carbonyl group indicated that the microorganisms present in the basal medium may be favoring chain scission PP generating hydrolysis product of grafted monomers. In addition, DSC results suggest that the biodegradation of polypropylene is occurring by enzymatic route, and being a semicrystalline polymer, it starts in the amorphous zones, to reach in a second stage the crystalline zones. The increase in the degree of crystallinity is a product of the degradation that is occurring faster in the amorphous regions than in the crystalline regions.

Acknowledgments

Thanks to FONACIT for financing this research under number F-201300395, to Fundación POLAR for the donation of the spectrometer FTIR and the Instituto de Investigaciones en Biomedicina y Ciencias Aplicadas "Dra. Susan Tai" (IIBCA), to Centro Regional de Investigaciones Ambientales (CRIA) of the Universidad de Oriente, Venezuela and to Prof. Alejandro Müller, *Ph.D* for his collaboration in supplying cassava starch and his valuable guidance in this work.

References and Notes

- [1] Mendes, J. F.; Paschoalin, R. T.; Carmona, V. B.; Neto, A. R. S.; Marques, A. C. P.; Marconcini, J. M.; Oliveira, J. E. *Carbohydr. Polym.* **2016**, *137*, 452. [\[Crossref\]](#)
- [2] Walker, A.; Tao, Y.; Torkelson, J. M. *Polymer* **2007**, *48*, 1066. [\[Crossref\]](#)
- [3] Fajardo, P.; Martins, J. T.; Fuciños, C.; Pastrana, L.; Teixeira, J. A.; Vicente, A. A. *J. Food Eng.* **2010**, *101*, 393. [\[Crossref\]](#)
- [4] Šimkovic, I. *Carbohydr. Polym.* **2013**, *95*, 697. [\[Crossref\]](#)
- [5] Bajer, D.; Kaczmarek, H.; Bajer, K. *Carbohydr. Polym.* **2013**, *98*, 477. [\[Crossref\]](#)
- [6] Fourati, Y.; Tarrés, Q.; Mutjé, P.; Boufi, S. *Carbohydr. Polym.* **2018**, *199*, 51. [\[Crossref\]](#)
- [7] Ramis, X.; Cadenato, A.; Salla, J. M.; Morancho, J. M.; Valles, A.; Contat, L. Ribes, A. *Polym. Degrad. Stab.* **2004**, *86*, 483. [\[Crossref\]](#)
- [8] Martins, A. B.; Santana, R. M. C. *Carbohydr. Polym.* **2016**, *135*, 79. [\[Crossref\]](#)
- [9] Rojas de Gáscue, B.; López, J.; Prin, J.; Hernández, G.; Reyes, Y.; Marcano, L.; López, F.; Puig, C.; Müller, A. *Interciencia* **2005**, *30*, 388. [\[Crossref\]](#)
- [10] Rivero, I. E.; Balsamo, V. Müller, A. J. *Carbohydr. Polym.* **2009**, *75*, 343. [\[Crossref\]](#)
- [11] Bhosale, R.; Singhal, R. *Carbohydr. Polym.* **2006**, *66*, 521. [\[Crossref\]](#)
- [12] Hadad, D.; Geresh, S.; Sivan, A. *J. Appl. Microbiol.* **2005**, *98*, 1093. [\[Crossref\]](#)
- [13] Benítez, A.; Sánchez, J.; Arnal, M.; Müller, A.; Rodríguez, O. Morales, G. *Polym. Degrad. Stab.* **2013**, *98*, 490. [\[Crossref\]](#)
- [14] Roy, M.; Gupta, R.; Bhattachary, S.; Parthasarathy, R. *J. Polym. Environ.* **2008**, *16*, 27. [\[Link\]](#)
- [15] Ammala, A.; Bateman, S.; Drean, K.; Petinakis, E.; Sangwan, P.; Wong, S.; Yuan, Q.; Yu, L.; Patrick, C.; Leongi, K. *Polym. Sci.* **2011**, *36*, 1015. [\[Crossref\]](#)
- [16] Nguyen, D. M.; Do, T. V. V.; Grillet, A. C.; Thuc, H. H.; Thuc, C. N. *Int. Biodeterior. Biodegrad.* **2016**, *115*, 257. [\[Crossref\]](#)
- [17] Knitter, M.; Dobrzyńska-Mizera, M. *Mech. Compos. Mater.* **2015**, *51*, 245. [\[Link\]](#)
- [18] Xu, W.; Ge, M.; He, P. *J. Polym. Sci., Part B: Polym. Phys.* **2002**, *40*, 408. [\[Crossref\]](#)
- [19] Nachtigall, S. M. B.; Neto, R. B.; Mauler, R. S. *Polym. Eng. Sci.* **1999**, *39*, 630. [\[Crossref\]](#)
- [20] Walker, A.; Tao, Y.; Torkelson, J. M. *Polymer* **2007**, *48*, 1066. [\[Crossref\]](#)
- [21] Masood, F.; Yasin, T.; Hameed, A. *Int. Biodeterior. Biodegrad.* **2013**, *87*, 1. [\[Crossref\]](#)
- [22] Shah, A. A.; Hasan, F.; Hameed, A.; Ahmed, S. *Biotechnol. Adv.* **2008**, *26*, 246. [\[Crossref\]](#)
- [23] Lorenzo, A. T.; Sabino, M. A.; Müller, A. J. *Revista Latinoamericana de Metalurgia y Materiales* **2003**, *23*, 25. [\[Link\]](#)
- [24] Sabino, M. A.; Albuérne, J.; Müller, A. J.; Brisson, J.; Prud'homme, R. E. *Biomacromolecules* **2004**, *5*, 358. [\[Crossref\]](#)
- [25] Sabino, M. A.; González, S.; Márquez, L.; Feijoo, J. L. *Polym. Degrad. Stab.* **2000**, *69*, 209. [\[Crossref\]](#)
- [26] Oder, G. *Structural Investigations of Polymers*, New York. Ellis Horwood, 1991.